Prognostic significance of fibroblast senescence and senescence-associated secretory phenotype factor expression in the tumor microenvironment of pancreatic ductal adenocarcinoma

YUTO KITANO[1], TOMOHARU MIYASHITA[1], TAKEO SHIMASAKI[2,3], ISAMU MAKINO[1], YOSHIO ENDO[4], YASUHIKO YAMAMOTO[5], NORIYUKI INAKI[6] and SHINTARO YAGI[1]

[1]Department of Hepato-Biliary-Pancreatic Surgery and Transplantation/Pediatric Surgery, Kanazawa University, Kanazawa, Ishikawa 920-8641, Japan; [2]Medical Research Institute, Kanazawa Medical University, Uchinada, Ishikawa 920-0293, Japan; [3]Department of Gastroenterological Endoscopy, Kanazawa Medical University, Uchinada, Ishikawa 920-0293, Japan; [4]Central Research Resource Branch, Cancer Research Institute, Kanazawa University, Kanazawa, Ishikawa 920-1192, Japan; [5]Department of Biochemistry and Molecular Vascular Biology, Graduate School of Medical Sciences, Kanazawa University, Kanazawa, Ishikawa 920-8641, Japan; [6]Department of Gastrointestinal Surgery/Breast Surgery, Kanazawa University, Kanazawa, Ishikawa 920-8641, Japan

Received April 29, 2025; Accepted October 16, 2025

DOI: 10.3892/or.2025.9031

Abstract. Pancreatic ductal adenocarcinoma (PDAC) is characterized by a dense fibrous stroma, within which a subset of fibroblasts function as cancer-associated fibroblasts (CAFs) and contribute to tumor progression. Some of these fibroblasts undergo senescence and promote malignancy through the senescence-associated secretory phenotype (SASP). The present study investigated SASP factor expression in senescent fibroblasts within the PDAC microenvironment and evaluated their impact on tumor progression. The expression levels of the senescence marker p16 and the SASP factor interleukin-6 (IL-6) were assessed using fluorescence immunostaining in resected specimens from 90 patients with PDAC who underwent pancreaticoduodenectomy. Senescence was induced in primary human pancreatic fibroblasts via X-ray irradiation *in vitro*, followed by evaluation of SASP factor expression. These senescent fibroblasts were then co-cultured with human pancreatic cancer Panc-1 cells to assess their effects on cancer cell invasion, migration and proliferation. Immunostaining demonstrated the presence of p16- and IL-6-expressing fibroblasts in the PDAC stroma of patient samples. A positive correlation was observed between p16 and IL-6 expression levels in fibroblasts. Notably, increased expression levels of IL-6-positive fibroblasts were associated with reduced postoperative survival. Multivariate analysis identified high IL-6 expression and lymph node metastasis as independent prognostic indicators of poor outcome. In co-culture experiments, senescent fibroblasts enhanced Panc-1 cell invasion, migration and proliferation. These findings suggested that senescent fibroblasts within the PDAC stroma, with high SASP factor expression, contribute to tumor aggressiveness and are associated with poor prognosis. The present study demonstrated that IL-6-expressing senescent fibroblasts are potential prognostic markers and therapeutic targets in PDAC, therefore the targeted elimination of senescent cells may represent a promising therapeutic strategy.

Introduction

In healthy proliferative cells, irreversible growth arrest is induced when irreparable DNA damage occurs as a result of telomere shortening, oncogene activation, excessive oxidative stress; this state is referred to as cellular senescence (1-3). Senescent cells have been observed *in vivo* and are recognized as a physiological phenomenon (4-7). Key features of senescent cells include permanent cell cycle arrest, morphological changes such as cellular enlargement and flattening, formation of senescence-associated heterochromatic foci, activation of senescence-associated β-galactosidase (SA-β-gal) and upregulation of the cell cycle inhibitors p21 and p16 (3). Similar to apoptosis, cellular senescence is considered an important tumor-suppressive mechanism that prevents abnormal proliferation and cancer development (8,9). However, studies have shown that senescent cells not only cease proliferating but can also persist for extended periods, contributing to a phenomenon known as the senescence-associated secretory phenotype (SASP) (5,8,9). The SASP involves the elevated secretion of various bioactive molecules with pro-tumorigenic effects, including inflammatory cytokines, chemokines, extracellular

Correspondence to: Dr Tomoharu Miyashita, Department of Hepato-Biliary-Pancreatic Surgery and Transplantation/Pediatric Surgery, Kanazawa University, 13-1 Takara-machi, Kanazawa, Ishikawa 920-8641, Japan
E-mail: tomoharumiya@gmail.com

Key words: pancreatic ductal adenocarcinoma, prognosis, senescence, fibroblasts, senescence-associated secretory phenotype

matrix-remodeling enzymes and growth factors (8). Although SASP factors serve physiological roles in processes such as tissue development and wound healing, excessive accumulation of senescent cells and SASP factors may have detrimental effects. These include the development of age-related diseases such as atherosclerosis, induction of chronic inflammation and promotion and progression of cancer (10,11). Thus, although cellular senescence serves as a short-term cancer-suppressive mechanism, its long-term presence and associated SASP may contribute to carcinogenesis and tumor progression. These findings suggest that cellular senescence has a dual nature: Protective in the short term, yet potentially harmful over time (Fig. 1) (8,9,11).

Senescent cells exhibit morphological changes, appearing larger and more flattened than proliferating cells. They accumulate dysfunctional mitochondria and display elevated levels of reactive oxygen species (ROS). Lysosomal content is increased, reflected by enhanced β-galactosidase activity in acidic environments (pH 6.0). Cells exhibiting the SASP secrete a wide array of factors that promote angiogenesis, extracellular matrix remodeling, epithelial-mesenchymal transition and tumor-promoting activities (12). Chronic inflammation induced by senescent cells may also lead to immunosuppression, contributing to cancer development and age-related diseases (10,11).

The tissue microenvironment is shaped by the physical and chemical influences of resident and surrounding cells, along with local factors such as growth factors, cytokines, temperature and oxygen levels (8). In cancerous tissues, the tumor microenvironment is composed of various cells and signaling molecules that surround cancer cells and promote tumor progression and invasion. Among these, certain fibroblasts function as cancer-associated fibroblasts (CAFs) (13-16). Studies suggest that a CAF-rich tumor microenvironment contributes to cancer invasion, metastasis, immune evasion and drug resistance (17,18). Stromal depletion through chemotherapy has been shown to improve drug resistance in cancer (19,20). Furthermore, senescence and SASP expression have been observed in fibroblasts within the stroma of several solid tumors (such as hepatocellular carcinoma, ovarian cancer, and prostate cancer) and are thought to influence tumor progression, suggesting these are common features across tumor types (21-23). Notably, pancreatic ductal adenocarcinoma (PDAC) and diffuse type gastric cancer are characterized by abundant fibrous stroma and particularly poor prognoses (24,25). However, the current understanding of stromal senescence and SASP expression in PDAC or their prognostic relevance is limited.

The present study focused on PDAC, which is particularly characterized by a dense fibrotic stroma among types of digestive system cancer. Using resected specimens from patients with PDAC, the present study aimed to investigate the presence of senescent fibroblasts and SASP factor expression in the tumor stroma, and their association with cancer progression and patient prognosis. Furthermore, senescent human pancreatic fibroblasts were established and co-cultured with pancreatic cancer cells with the aim of evaluating the effects of SASP on tumor cell behavior. Elucidating the impact of stromal senescence and SASP expression on patient prognosis in PDAC may help identify novel prognostic biomarkers and therapeutic targets, potentially leading to the development of stroma-targeted treatments for this aggressive cancer.

Materials and methods

Patients and pancreatic tissue. The present study utilized 90 resected specimens from patients who underwent pancreaticoduodenectomy for PDAC involving the pancreatic head at Kanazawa University Hospital between 2006 and 2017; retrospective study was conducted on patients treated between 2006 and 2015. The study protocol was approved by the Ethics Committee of Kanazawa University Hospital (approval no. 2016-318; Kanazawa, Japan), and complied with the Declaration of Helsinki (1975) and the Ethical Guidelines for Medical and Biological Research Involving Human Subjects by the Japanese Government (26). Written informed consent was obtained from all participants for the anonymous use of resected specimens and clinical data. The clinical characteristics of the patients were as follows: Median age, 66 years (age range, 35-81); sex distribution, male (62%) and female (38%); pathological stage of PDAC based on the Union for International Cancer Control (8th edition) TNM classification (27): Stage I, n=34; stage II, n=31; and stage III, n=25; and preoperative chemotherapy in 59 cases (66%). Of the total cohort, 1 patient received preoperative radiation therapy. All patients were followed up after surgery for up to 8 years, and survival was defined as the time from pancreaticoduodenectomy to death or the last visit to the hospital.

Immunohistochemistry and immunofluorescence. Paraffin-embedded sections of 4-μm thickness (10% neutral buffered formalin-fixed for 24 h at room temperature) were prepared for immunohistochemistry and immunofluorescence. The Dako Envision system (Dako; Agilent Technologies, Inc.), which uses dextran polymers conjugated to horseradish peroxidase, was employed for immunohistochemical and immunofluorescent staining to avoid any endogenous biotin contamination. Sections were deparaffinized in xylene and rehydrated in a graded ethanol series. Endogenous peroxidase was blocked by immersing sections in 3% H_2O_2 in 100% methanol for 20 min at room temperature (~26˚C). Antigen retrieval was achieved by microwaving sections at 95˚C for 10 min in 0.001 M citrate buffer (pH 6.7). After blocking endogenous peroxidase, sections were incubated with Protein Block Serum-Free (Dako; Agilent Technologies, Inc.) at room temperature (~26˚C) for 10 min to block non-specific staining.

Fibroblasts in the pancreatic cancer stroma were identified via immunohistochemistry and immunofluorescence staining with a mouse monoclonal anti-a smooth muscle actin (αSMA; cat. no. ab7817; Abcam) antibody. A rabbit polyclonal anti-CDKN2A/p16INK4a (cat. no. ab189034; Abcam) antibody and a mouse monoclonal anti-interleukin-6 (IL-6; cat. no. ab9324; Abcam) antibody were used to identify p16- and IL-6-positive fibroblasts within the PDAC stroma. Primary antibodies were applied for 2 h at room temperature (~26˚C). The fluorescent dyes used were goat anti-mouse IgG H&L (Alexa Fluor 488; cat. no. ab150113; Abcam), donkey

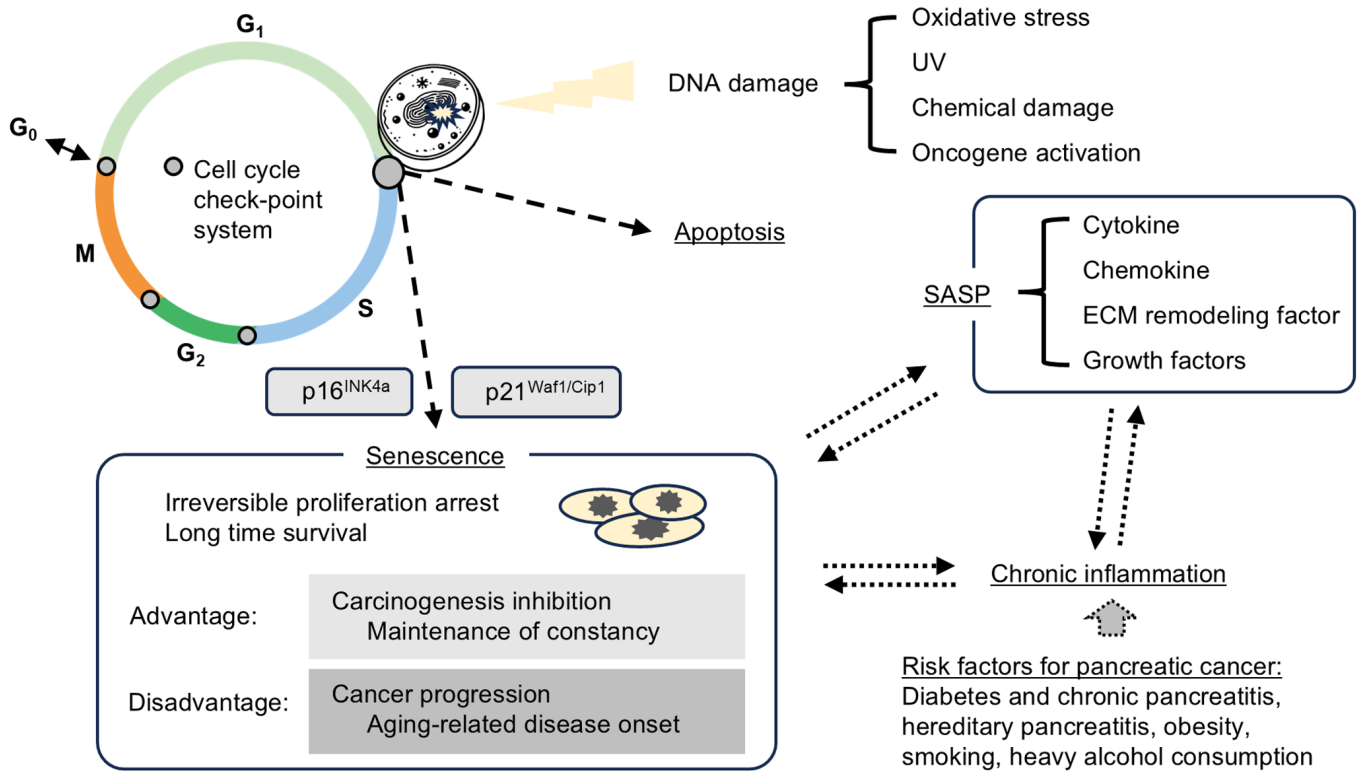

Figure 1. Molecular mechanisms of cellular senescence. DNA damage induces cellular senescence, characterized by either apoptosis or irreversible cell cycle arrest. Senescent cells release SASP factors, which promote chronic inflammation and are involved in carcinogenesis and the development of age-related diseases. SASP, senescence-associated secretory phenotype.

anti-rabbit IgG H&L (Alexa Fluor 647; cat. no. ab150075; Abcam) and DAPI (cat. no. ab104139; Abcam). Secondary antibodies were applied for 1 h at room temperature (~26˚C).

When staining culture plates, cells were fixed with 4% paraformaldehyde for 15 min, permeabilized with 0.05% Triton X-100 in 1X PBS for 15 min and blocked with 1% fetal bovine serum (FBS; Nichirei Biosciences, Inc.) in 1X PBS for 30 min at room temperature (~26˚C). A mouse monoclonal anti-AE1/AE3 (cat. no. sc-81714; Santa Cruz Biotechnology) antibody and a mouse monoclonal anti-Vimentin (cat. no. sc-6260; Santa Cruz Biotechnology) antibody were used to identify established human pancreatic fibroblasts. Primary antibodies were applied for 2 h at room temperature (~26˚C). Peroxidase activity was detected using the enzyme substrate DAB. Samples were counterstained with hematoxylin for 1 min or DAPI for 30 min at room temperature (~26˚C).

The mean expression intensities of p16- and IL-6-positive fibroblasts were quantified by counting three fields per specimen (magnification, x100). To evaluate expression levels quantitively, H-score analysis was employed (28,29). Immunohistochemical images were captured using an optical microscope (BX-50; Olympus Corporation), and fluorescent images were captured using a BZ-X710 microscope (Keyence Corporation).

Establishment of human pancreatic fibroblasts. A human pancreatic fibroblast cell line was established using a resected pancreatic specimen of the non-tumorous area from a patient with pancreatic cancer, performed as previously described (30,31). To maintain sterility, pancreatic tissue from the non-tumorous area (~5 μm^3) with adequate margin was collected under clean conditions. The tissue was minced using scissors and cultured in Dulbecco's Modified Eagle Medium (DMEM; Nacalai Tesque, Inc.) supplemented with 10% FBS in a 10-cm culture dish. After 3-4 days of incubation at 37˚C, proliferation of bipolar or multipolar spindle-shaped cells was observed, whereas no proliferation was seen in cell populations with other morphologies. Pancreatic fibroblasts were successfully established based on cell morphology and marker expression; spindle-shaped cells tested positive for αSMA and vimentin by immunostaining. Fibroblasts between passages 4 and 8 were used.

Cell lines and culture conditions. The Panc-1 cell line, derived from human pancreatic cancer cells (cat. no. CRL-1469; American Type Culture Collection) was used in the present study. Pancreatic cancer cell lines and pancreatic fibroblasts were cultured in DMEM supplemented with 10% FBS at 37˚C in a humidified atmosphere with 5% CO_2. The culture medium was replaced 2-3 times per week.

Induction of cellular senescence in human pancreatic fibroblasts. Confluent monolayers of human pancreatic fibroblasts cultured in 6-well plates were irradiated with X-rays at a dose of 10 Gy. The fibroblasts were maintained using the culture conditions described above, with medium changes every 3 days. On days 0, 3, 6 and 9 after irradiation, SA-β-gal staining was performed using a Cellular Senescence Kit (OZ Biosciences) according to the manufacturer's instructions to

evaluate cellular senescence. To assess the dose-dependent induction of senescence, fibroblasts were irradiated at 3, 6 and 10 Gy, and SA-β-gal staining was performed on day 9 after irradiation. Fibroblasts irradiated with 10 Gy in 6-cm culture dishes were collected on day 9 post-irradiation for further analysis.

Real-time PCR. Total mRNA was extracted using TRIzol reagent (Thermo Fisher Scientific, Inc.) and reverse transcription was performed using the AffinityScript QPCR cDNA Synthesis Kit (Agilent Technologies, Inc.) according to the manufacturer's protocol. Reverse transcription-quantitative PCR (RT-qPCR) was conducted using an Mx3000P system (Agilent Technologies, Inc.) with a SYBR Green PCR Kit (Qiagen GmbH) in triplicate, using specific primers. The primer sequences used to assess target gene expression were as follows: IL-6, forward (F), 5'-ATGAACTCCTTCTCC ACAAGC-3' and reverse (R), 5'-GTTTTCTGCCAGTGCCTC TTTG-3'; IL-1, F, 5'-ATCAGTACCTCACGGCTGCT-3' R, 5'-TGGGTATCTCAGGCATCTCC-3'; IL-8 F, 5'-AACATG ACTTCCAAGCTGGC-3' R, 5'-AAACTTCTCCACAAC CCTCTGC-3'; MMP-1 F, 5'-AGCTAGCTCAGGATGACA TTGATG-3' R, 5'-GCCGATGGGCTGGACAG-3'; VEGF F, 5'-ATGAACTTTCTGCTGTCTTGGGT-3' R, 5'-TGGCCT TGGTGAGGTTTGATCC-3'; p16 F, 5'-CCCAACGCACCG AATAGTTA-3' R, 5'-ACCAGCGTGTCCAGGAAG-3'; and GAPDH F, 5'-GACAGTCAGCCGCATCTTCT-3' R, 5'-TTA AAAGCAGCCCTGGTGAC-3' The following thermocycling conditions were used for qPCR: Initial denaturation at 95˚C for 10 min; 40 cycles of denaturation at 95˚C for 30 sec; annealing at 55˚C for 1 min; and extension at 72˚C for 1 min. Real-time PCR was conducted according to the $2^{-\Delta\Delta Cq}$ method (32), with GAPDH as the internal control.

Western blotting. After collection, cells were lysed on ice in RIPA lysis buffer (Wako Pure Chemical Industries, Ltd.) containing a protease inhibitor. Protein concentrations were measured using the Pierce BCA Protein Assay Kit (Thermo Fisher Scientific, Inc.). Total cellular proteins (20 μg) from each sample were separated by 12.5% gradient polyacrylamide gel electrophoresis (e-PAGEL; ATTO Corporation) and transferred onto a nitrocellulose membrane. Membranes were blocked with Odyssey Blocking Buffer (LI-COR Biosciences) for 2 h at 26˚C and incubated overnight at 4˚C with the primary antibodies. The following primary antibodies were used: p16 (1:1,000; cat. no. ab189034; Abcam), IL-6 (1:1,000; cat. no. ab9324; Abcam) and β-actin (1:10,000; cat. no. A5441; Sigma-Adrich; Merck KGaA), which served as the internal control. After three 10-min washes with Tris-buffered saline containing 0.05% of Tween 20, membranes were incubated for 1 h at 26˚C with either IRDye 680RD-conjugated goat anti-rabbit IgG (1:10,000; cat. no. 925-68071; LI-COR Biosciences) or IRDye 800CW-conjugated goat anti-mouse IgG (1:10,000; cat. no. 925-32210; LI-COR Biosciences). Western blot images were analyzed using an Odyssey infrared imaging system software (version 4.0; LI-COR Biosciences).

Matrigel invasion assay. A Corning Matrigel Invasion Chamber (cat. no. 354480; Corning, Inc.) in a 24-well plate format (cat. no. 353504; Corning, Inc.) was used and two groups of fibroblasts were prepared: Pancreatic fibroblasts collected 9 days after irradiation and non-irradiated pancreatic fibroblasts maintained in culture for the same duration (9 days). Matrigel precoating was performed at 37˚C for 1 h for the invasion assay. First, $1x10^5$ fibroblasts in 1 ml DMEM were seeded into the lower chamber. After 2 h, $5x10^4$ Panc-1 cells in 500 μl DMEM were added to the upper chamber to initiate co-culture (n=6). The culture medium used was DMEM supplemented with 10% FBS. After 24 h of incubation at 37˚C, the chambers were collected. Following gel removal, membranes were stained with hematoxylin for 2 min at 26˚C. The number of pancreatic cancer cells that had invaded through the membrane was counted under an optical microscope (BX-50, Olympus Corporation). As a control, Panc-1 cells were cultured in the upper chamber without fibroblasts in the lower chamber.

Scratch assay and application of culture supernatant. Pancreatic fibroblasts were cultured into confluent in 10-cm dishes containing (either 9 days post-irradiation or non-irradiated). After culturing the fibroblasts in DMEM supplemented with 1% FBS for 48 h at 37˚C, the culture supernatant was collected for use in subsequent experiments. Simultaneously, 6-well plates containing confluent monolayers of Panc-1 cells cultured in serum-free DMEM for 24 h at 37˚C were scratched using a pipette tip. The collected culture supernatants from irradiated and non-irradiated fibroblasts were added to the wells (2 ml/well), and the plates were incubated at 37˚C. After 24 h, the area into which Panc-1 cells had migrated was measured. As a control, scratched confluent monolayers of Panc-1 cells were cultured in serum-free DMEM not containing fibroblast culture supernatant. A microscope (BX-50, Olympus Corporation) was used for cell observation. Migration was quantified by comparing the final images with baseline images captured immediately after scratching (n=6), using the ImageJ software (version 1.51k; National Institutes of Health) (33). For each group, the cell migration area was calculated by subtracting the area of the cell-free region (scratch line) at 24 h from the area at 0 h. The cell migration area for the control group was set as 1, and the cell migration area for each group was calculated as a ratio.

Cell proliferation assay. Cell proliferation was measured using the MTT assay (n=8). Confluent monolayers of irradiated pancreatic fibroblasts in 10-cm dishes were cultured in DMEM supplemented with 1% FBS for 48 h, and the resulting culture supernatant was collected. Panc-1 cells were seeded at a density of 6,000 cells per well in 96-well plates, and 200 μl of the fibroblast supernatant, adjusted to contain 10% FBS, was added to each well. Cells were incubated for 24 and 48 h at 37˚C. After incubation, the medium was removed, and the crystallized formazan was solubilized by addition of dimethyl sulfoxide. Absorbance was measured at 535 nm using a microplate reader (Bio-Rad 550; Bio-Rad Laboratories, Inc.). Panc-1 cells cultured without the fibroblast supernatant were used as controls.

Statistical analysis. Statistical analyses were performed using EZR software (version 1.63; Saitama Medical Center;

Jichi Medical University). Demographic and clinicopathological characteristics were summarized using descriptive statistics. To compare characteristics between groups, the χ^2 test was used for categorical variables, and Student's t-test or one-way ANOVA followed by Turkey's post hoc test was used for unpaired continuous variables. Pearson's correlation coefficient (r) was used to assess correlations between the expression levels of p16- and IL-6-positive fibroblasts in the pancreatic cancer stroma, and between IL-6-positive fibroblast expression and postoperative survival time. Receiver operating characteristic (ROC) curve analysis was used to determine the IL-6 cut-off value for prognosis. Survival curves were generated using the Kaplan-Meier method and compared using the log-rank test. Multivariate analysis was performed using the Cox proportional hazards model on variables that showed significance in univariate analysis. Results are presented as mean ± standard deviation. All statistical tests were two-tailed. P<0.05 was considered to indicate a statistically significant difference.

Results

Assessment of PDAC stromal senescence and expression of SASP factors in PDAC specimens. Using resected pancreatic cancer specimens, the presence of senescent fibroblasts in the pancreatic cancer stroma and the expression of SASP factors were evaluated. αSMA was used as a marker for pancreatic fibroblasts (13,19). Although multiple proteins are known markers of cellular senescence (8,13,16), p16 expression levels were evaluated as its expression is extremely low in proliferating cells but increases markedly when cells reach their mitotic limit or are exposed to carcinogenic stress, inducing cellular senescence (34,35). Simultaneous immunofluorescence staining for αSMA and p16 revealed double-positive cells within the pancreatic cancer stroma, which confirmed the presence of fibroblasts exhibiting features of cellular senescence (Fig. 2A). Although various cytokines, chemokines, growth factors and extracellular matrix-degrading factors are recognized as SASP components, IL-6 was assessed as a representative and pleiotropic proinflammatory cytokine (8,9,13). The fibroblasts were positive for both p16 and IL-6 in the tumor stroma (Fig. 2B), indicating that senescent fibroblasts in the PDAC stroma express the SASP factor IL-6. Using resected pancreatic cancer specimens, immunohistochemistry with p16 and IL-6 targeting the pancreatic cancer stroma was then performed. A significant positive correlation was found between p16 and IL-6 expression (r=0.585, P<0.0001; Fig. 2C), which suggested that IL-6 expression increased proportionally with the number of senescent fibroblasts in the tumor stroma. Based on these findings, subsequent analyses on IL-6 expression in the PDAC stroma was conducted.

Postoperative prognosis according to IL-6 expression in the PDAC stroma. The association between IL-6 expression in stromal fibroblasts and overall survival (OS) following pancreaticoduodenectomy was investigated. A significant negative correlation was found between IL-6-positive fibroblast expression and postoperative survival (r=-0.336, P=0.0012; Fig. 3A). Therefore, it was considered that IL-6 expression in the tumor stroma may potentially serve as a prognostic factor after surgery. Using an ROC curve, the H-score cut-off value of 179 of IL-6 expression was determined to distinguish prognostic groups [area under the curve (AUC)=0.754, sensitivity=0.736 and specificity=0.734; Fig. 3B]. The H-score cut-off was used to patients divide into high- (≥179) and low-IL-6 (<179) expression groups and Kaplan-Meier analysis of OS of the two groups was performed. The high-IL-6 expression group demonstrated a significantly poorer OS compared with that of the low-IL-6 group (log-rank test, P=0.00002; Fig. 3C). IHC was performed on representative PDAC specimens with weak (Fig. 3D), moderate (Fig. 3E) and strong (Fig. 3F) IL-6 positivity, and a non-tumorous pancreatic specimen (Fig. 3G). Univariate analysis identified curability, T factor (T3 or T4), lymph node metastasis, neuroplexus invasion and high-IL-6 expression as significant prognostic factors. Multivariate analysis further confirmed lymph node metastasis and high IL-6 expression as independent prognostic indicators (Table I). Patient demographics and clinicopathological characteristics of high- and low-IL-6 expression groups are summarized in Table II. There were no significant differences between groups in terms of baseline characteristics, including preoperative chemotherapy, combined portal vein or arterial resection and curative resection. The high IL-6 expression group demonstrated a notably higher proportion of patients with advanced T and N classifications compared with that of the low-expression group, although this not statistically significant. To evaluate whether patient characteristics or tumoral factors influenced IL-6 expression in stromal fibroblasts of PDAC, a subgroup analysis was conducted. Stromal IL-6 expression was not associated with any patient characteristics or tumoral factors (Table III). In this cohort, neither patient age nor preoperative chemotherapy were associated with IL-6 expression in senescent stromal fibroblasts.

Induction of cellular senescence in established human pancreatic fibroblasts and co-cultures with PDAC cell lines. Hematoxylin and eosin staining of cells established from resected pancreatic specimens was used to confirm the proliferation of bipolar or multipolar spindle-shaped cells with basophilic nuclei and cytoplasm. AE1/3 staining was negative, whereas αSMA and vimentin were diffusely positive (Fig. 4A), which demonstrated the successful isolation of pancreatic fibroblasts from pancreatic specimens. Next, cellular senescence in the established pancreatic fibroblasts was induced. Cells were exposed to 10 Gy X-ray irradiation to induce DNA damage, and changes were observed over time by every 3 days (up to 9 days) post irradiation. The irradiated fibroblasts gradually ceased proliferation and exhibited cell and nuclear enlargement, which are hallmarks of senescent cells, and exhibited positive SA-β-gal staining (Fig. 4B), which indicated that radiation-induced DNA damage successfully induced cellular senescence in pancreatic fibroblasts. To assess the degree of senescence, a dose-gradient approach (3, 6 and 10 Gy irradiation) was applied. SA-β-gal staining was performed 9 days after irradiation. With increasing radiation doses, fibroblasts appeared flattened and exhibited enhanced SA-β-gal staining (Fig. 4C). Based on these temporal and dose-dependent findings, fibroblasts that were irradiated with 10 Gy and cultured for 9 days were used in subsequent experiments. The

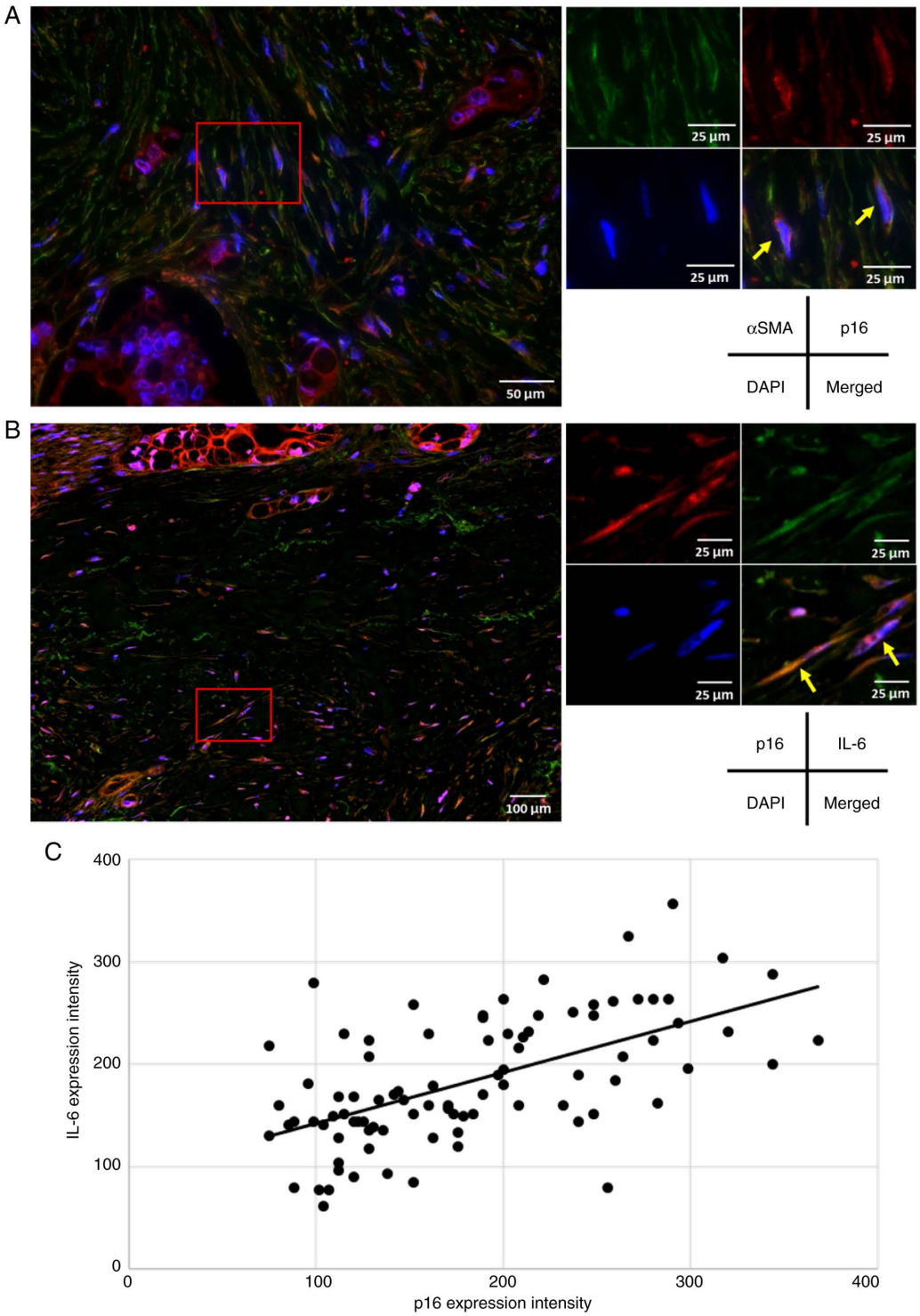

Figure 2. Evaluation of p16- and IL-6-positive cells in the stroma of pancreatic ductal adenocarcinoma. (A) Representative immunofluorescence staining of a pancreatic cancer resection specimen (αSMA, green; p16, red; DAPI, blue; scale bar, 50 and 25 μm). In the pancreatic cancer stroma, pancreatic fibroblasts (αSMA-positive) expressing the senescence marker p16 were identified (yellow arrows). (B) Representative immunofluorescence staining of a pancreatic cancer resection specimen (p16, red; IL-6, green; DAPI, blue; scale bar, 100 and 25 μm). Fibroblasts positive for p16 and the senescence-associated secretory phenotype factor IL-6 were observed in the pancreatic cancer stroma (yellow arrows). (C) A significant positive correlation between the expression intensity of p16- and IL-6-positive fibroblasts in the pancreatic cancer stroma (Pearson's correlation coefficient, r=0.585; P<0.0001).

expression levels of p16INK4a, as a marker of senescence in the fibroblasts, were then evaluated. Western blotting demonstrated no p16 expression in non-irradiated cells; however, irradiated fibroblasts showed consistently increased p16 expression from day 3 onward (Fig. 4D). Regarding the SASP factor IL-6, western blotting demonstrated a gradual increase in IL-6 protein expression beginning on day 3 (Fig. 4E), paralleled by a similar significant increase in IL-6 mRNA levels as confirmed by RT-qPCR (Fig. 4F). Immunofluorescence analysis on day 9 post-irradiation demonstrated cytoplasmic IL-6 staining in pancreatic fibroblasts (Fig. 4G). Additionally, the mRNA expression of other SASP components, including

Table I. Factors associated with overall survival in operated patients with pancreatic ductal adenocarcinoma.

	Univariate analysis			Multivariate analysis		
Factor	HR	95% CI	P-value	HR	95% CI	P-value
Age, ≥65 years			0.401			
Sex, male			0.748			
Neoadjuvant chemotherapy			0.838			
Curability (R1 or 2)	2.173	1.372-3.441	0.001	1.214	0.670-2.107	0.490
Histological differentiation[a]			0.119			
Tumor factor[a]						
T3 or 4	2.671	1.445-4.938	0.002	2.101	0.860-5.135	0.104
N1 or 2	4.607	2.411-8.806	0.00001	3.594	1.636-7.893	0.001
Histopathological factor						
Lymphatic invasion			0.516			
Vascular invasion			0.102			
Neuroplexus invasion	2.025	1.181-3.473	0.010	1.576	0.835-2.972	0.160
High IL-6 expression	4.486	2.564-7.846	0.00001	3.483	1.519-6.852	0.001

[a]According to Union for International Cancer Control (8th), CI, confidence interval; HR, hazard ratio.

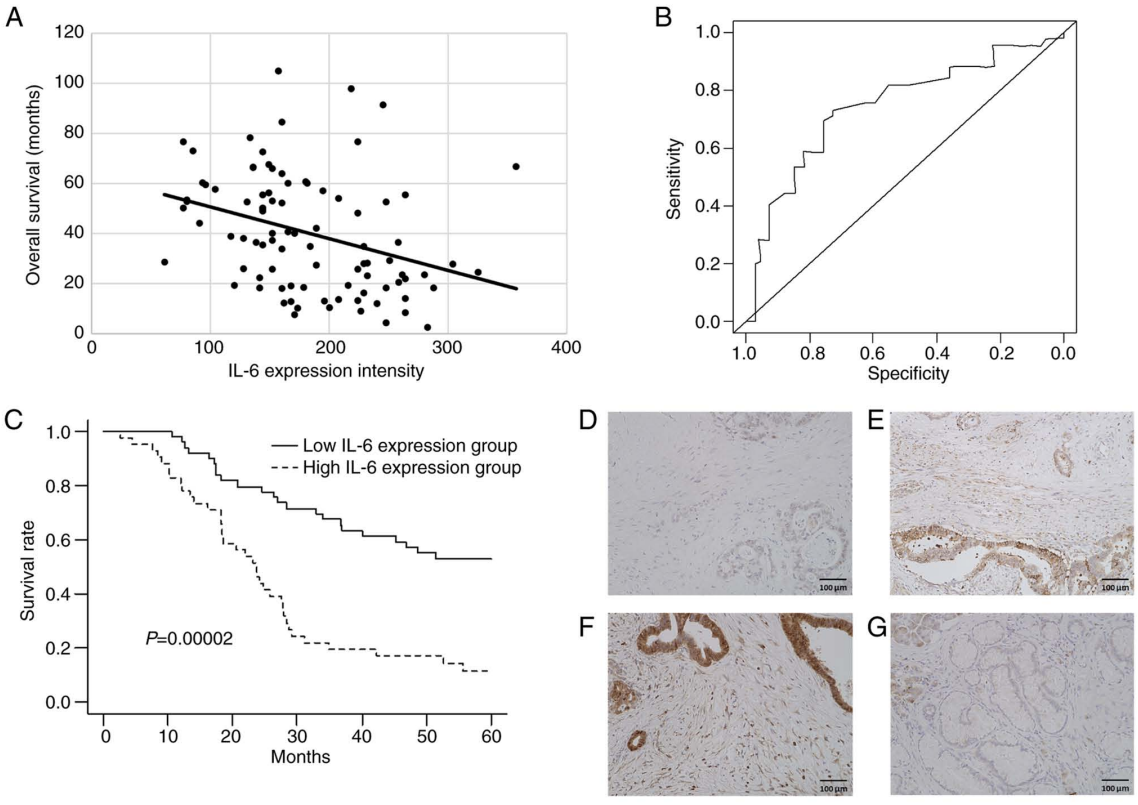

Figure 3. Relationship between IL-6 expression intensity in the pancreatic ductal adenocarcinoma stroma and prognosis after pancreaticoduodenectomy. (A) A significant negative correlation between the expression intensity of IL-6-positive fibroblasts in the pancreatic cancer stroma and overall survival (Pearson's correlation coefficient, r=-0.336; P=0.0012). (B) A receiver operating characteristic curve based on the expression intensity of IL-6-positive fibroblasts in the pancreatic cancer stroma and overall survival (AUC=0.754, sensitivity=0.736, specificity=0.734). The IL-6 H-score cut-off value was 179; patients with H-scores <179 were defined as the IL-6 low expression group, and those with scores ≥179 as the IL-6 high expression group. (C) Survival curves for patients with pancreatic cancer with low (solid line) and high (dotted line) -IL-6 expression (log-rank test, P=0.00002). Representative pancreatic cancer specimen with (D) weak, (E) moderate and (F) strong IL-6 positivity (scale bar, 100 μm). (G) Non-tumorous pancreatic specimen (scale bar, 100 μm).

cytokines (IL-1), chemokines (IL-8), extracellular matrix remodeling factors (MMP-1 and PAI-1) and a growth factor (VEGF) were assessed; these SASP components were significantly upregulated in irradiated fibroblasts (Fig. S1).

Table II. Relationship between stromal IL-6 expression and clinicopathological factors.

Characteristic	Low IL-6 expression, n	High IL-6 expression, n	P-value
Total patients	49	41	
Age, years			0.623
<65	30	23	
≥65	19	18	
Sex			0.823
Male	31	25	
Female	18	16	
Neoadjuvant chemotherapy			0.957
Present	32	27	
Absent	17	14	
Portal vein resection			0.317
Present	31	30	
Absent	18	11	
Artery resection			0.525
Present	4	5	
Absent	45	36	
Curability			0.828
R0	38	31	
R1/2	11	10	
T category[a]			0.189
T1/2	41	33	
T3/4	8	8	
N category[a]			0.156
N0	24	12	
N1	14	15	
N2	11	14	
UICC stage[a]			0.267
I	22	12	
II	16	15	
III	11	14	
Histological differentiation[a]			0.449
Well	10	6	
Moderate	34	32	
Poor	7	3	
Lymphatic invasion			0.881
Present	45	38	
Absent	4	3	
Vascular invasion			0.361
Present	41	37	
Absent	8	4	
Neuroplexus invasion			0.365
Present	24	24	
Absent	25	17	

[a]According to UICC (8th). UICC, Union for International Cancer Control.

These results suggested that radiation-induced DNA damage triggered cellular senescence and promoted SASP factor expression in pancreatic fibroblasts.

Invasive, migratory and proliferative capacities of Panc-1 cells with irradiated human pancreatic fibroblasts or culture supernatant. The invasive potential of Panc-1 cells

Table III. Subgroup analysis of the association with IL-6 expression in stromal fibroblasts was performed.

Factor	Hazard ratio	95% CI	P-value
Age (≥65 years)	0.749	0.293-1.910	0.546
Sex (male)	0.800	0.312-2.050	0.643
Neoadjuvant chemotherapy	0.963	0.364-2.540	0.939
Curability (R1 or 2)	0.731	0.301-1.780	0.491
Histological differentiation[a] (moderate or poor)	0.947	0.232-3.860	0.939
Tumor factor[a]			
T3 or 4	0.904	0.278-2.930	0.867
N1 or 2	2.680	0.901-7.960	0.076
Histopathological factor			
Lymphatic invasion	0.440	0.047-4.110	0.471
Vascular invasion	2.370	0.387-14.600	0.350
Neuroplexus invasion	1.190	0.433-3.300	0.731

[a]According to Union for International Cancer Control (8th). CI, confidence interval.

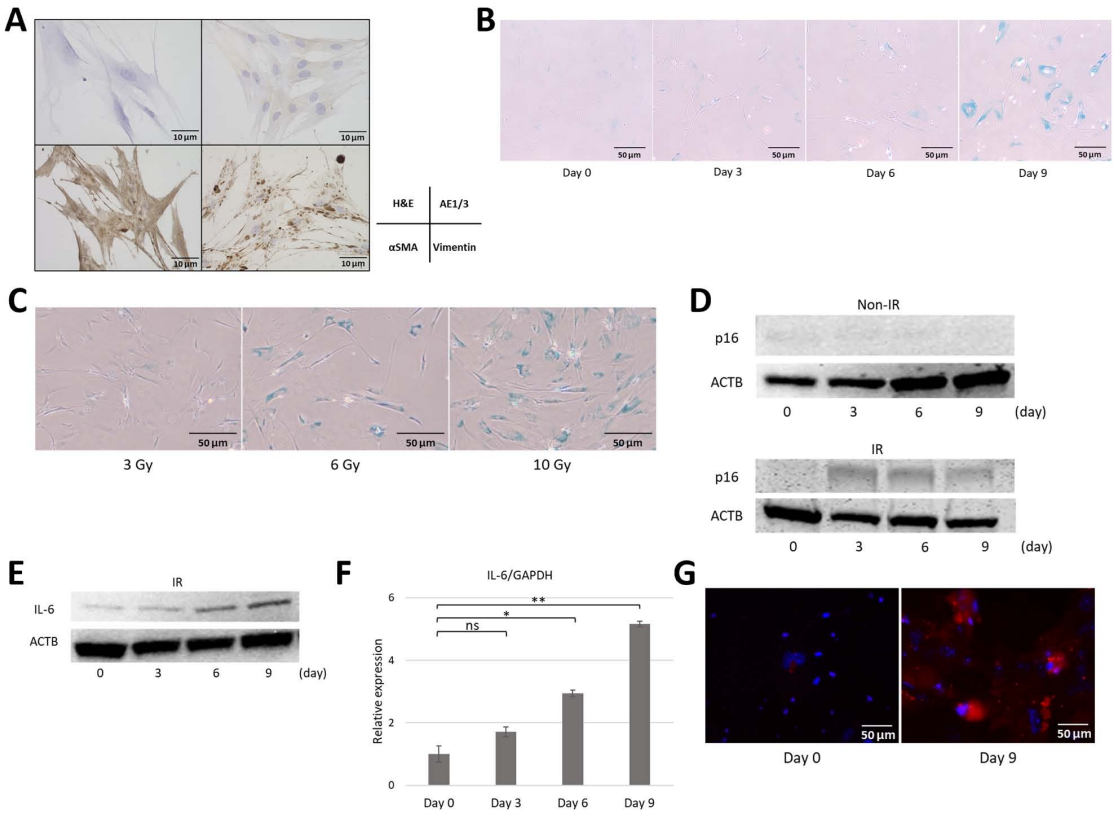

Figure 4. Establishment of human pancreatic fibroblast cell lines and induction of cellular senescence and the senescence-associated secretory phenotype. (A) Pancreatic fibroblasts established from resected pancreatic specimens. Cells showed a spindle-shaped morphology with cytoplasmic protrusions (AE1/3-negative, αSMA- and vimentin-positive; scale bar, 10 μm). (B) SA-β-gal staining of IR pancreatic fibroblasts (10 Gy) increased over time (scale bar, 50 μm). (C) SA-β-gal staining of pancreatic fibroblasts 9 days increased with gradient irradiation (3, 6 and 10 Gy; scale bar, 50 μm). (D) Western blot analysis of p16 protein expression in IR pancreatic fibroblasts (10 Gy X-rays on days 0, 3, 6 and 9) showed increased p16 protein expression from day 3 onward compared with the non-IR group. (E) Western blot analysis showed a gradual increase of IL-6 protein expression from day 3 onwards to day 9 post-irradiation. (F) Reverse transcription-quantitative PCR confirmed increased IL-6 mRNA expression after irradiation over 9 days of culture. Data are presented as mean ± SD (n=6). (G) Immunofluorescence of pancreatic fibroblasts. IL-6 expression was increased on day 9 (IL-6, red; DAPI, blue; scale bar, 50 μm). *P<0.01 and **P<0.001. ns, not significant; H&E, hemoxylin and eosin; SA-β-gal, senescence-associated β-galactosidase; aSMA, a smooth muscle actin; ACTB, β-actin; IR, irradiated.

co-cultured with fibroblasts 9 days post-irradiation was evaluated. Panc-1 cells were co-cultured with fibroblasts, and the number of cancer cells that migrated through the Matrigel and membrane was quantified. Co-culture with pancreatic

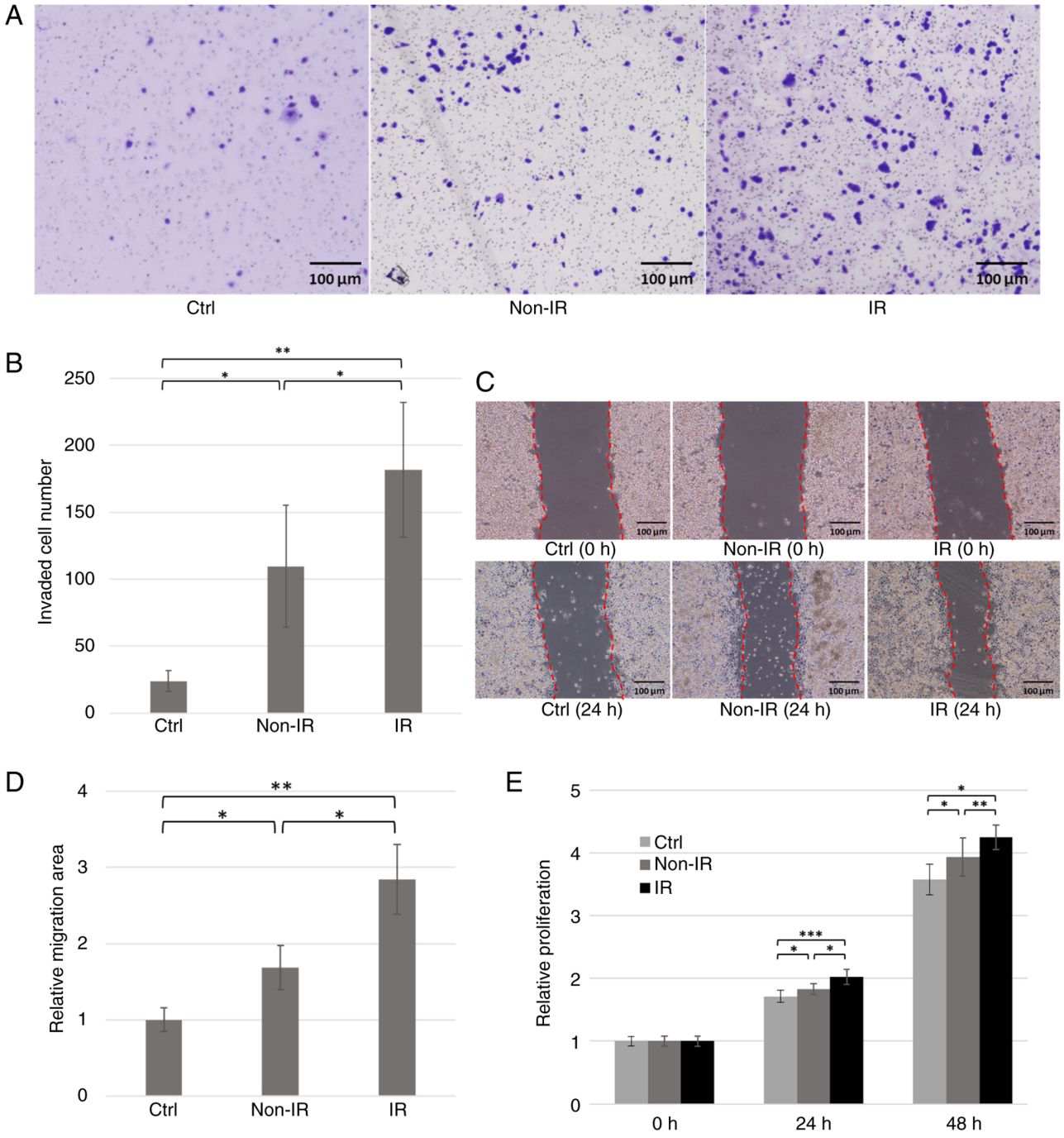

Figure 5. Co-culture experiments of Panc-1 cells with IR human pancreatic fibroblasts or their culture supernatants. (A) Representative images of pancreatic fibroblasts (10 Gy IR or non-IR) that were co-cultured with Panc-1 cells (scale bar, 100 μm), and (B) the number of cells that invaded through the gel and membrane was counted (n=6). (C) A confluent monolayer of Panc-1 cells was scratched with a pipette, and the culture supernatant of IR or non-IR pancreatic fibroblasts was added (scale bar, 100 μm). (D) After 12 h, the area of cell migration was measured (n=6). *P<0.05 and **P<0.01. (E) Panc-1 cells were cultured with culture supernatants of IR or non-IR pancreatic fibroblasts, and proliferation was assessed after 24 and 48 h using the MTT assay (n=8). Data are presented as mean ± SD. *P<0.05, **P<0.01 and ***P<0.001. aSMA, a smooth muscle actin; Ctrl, control; IR, irradiated.

fibroblasts significantly enhanced Panc-1 invasion compared with that of control cells, and this effect was further amplified by co-culture with irradiated, SASP-expressing fibroblasts (Fig. 5A and B).

Panc-1 cells were cultured in the conditioned medium from irradiated or non-irradiated fibroblasts, and their migration capacity was evaluated. The groups treated with conditioned medium showed significantly larger migration areas compared with control. Furthermore, the group treated with conditioned medium from irradiated, SASP-expressing fibroblasts showed a significantly larger migration area compared with that of cells treated with medium from non-irradiated fibroblasts (Fig. 5C and D).

Cell proliferation of Panc-1 cells was assessed using the MTT assay (n=8). Panc-1 cells cultured in fibroblast-conditioned medium exhibited significantly higher proliferation compared with those cultured in standard serum-containing medium. Furthermore, conditioned medium from irradiated fibroblasts

demonstrated significantly increased Panc-1 proliferation compared with cells treated with either serum-containing medium or medium from non-irradiated fibroblasts (Fig. 5E). These findings indicated that pancreatic fibroblasts expressing the SASP significantly enhanced the proliferative capacity of pancreatic cancer cells.

Discussion

Research has shown that cells and molecules within or around the cancer stroma form the cancer microenvironment in various carcinomas. Furthermore, the fibrous stroma serves an important role in shaping the cancer microenvironment (13-16). In particular, cellular senescence of the fibrotic stroma and the expression of SASP factors associated with cellular senescence have been reported to significantly impact cancer progression in several carcinomas (such as hepatocellular carcinoma, ovarian and prostate cancer) (21-23). In gastrointestinal carcinomas, pancreatic ductal and diffuse-type gastric cancer have a more abundant fibrotic stroma than other malignant tumors of the digestive tract and are known to have poor prognoses (24,25).

Certain underlying health conditions and lifestyle factors are risk factors for pancreatic cancer, including diabetes, chronic pancreatitis, hereditary pancreatitis, obesity, smoking and heavy drinking (36-39). These are also risk factors for chronic inflammation, whereas obesity, smoking and alcohol consumption are known risk factors for other types of malignancies (40-43). This suggests that systemic and/or local chronic inflammation in the pancreas caused by underlying diseases and/or lifestyle factors induces cellular senescence and SASP in the pancreatic stroma, and that oxidative stress, DNA damage and oncogene activation occur in the pancreatic stroma before pancreatic cancer develops. After carcinogenesis, various cytokines, chemokines and reactive oxygen species produced by cancer cells interact with the surrounding stroma, inducing further fibroblast production and forming a desmoplastic microenvironment (13,17).

The status of lymph node metastasis is widely recognized as an important prognostic factor for pancreatic cancer and is reflected in the TNM classification of cancer staging (27,44). In the present study, multivariate analysis using the Cox proportional hazards model indicated that lymph node metastasis and high IL-6 expression were significant prognostic factors. The presence of fibroblasts positive for p16 and IL-6, representative SASP factors, was confirmed in the stroma of resected PDAC specimens. These results suggested that senescent fibroblasts exist in the pancreatic cancer stroma and express SASP factors. The expression intensity of IL-6-positive cells in the pancreatic cancer stroma was calculated using H-score analysis, and a cut-off value of 179 was defined using an ROC curve. Based on this cut-off value, it was demonstrated that the OS of patients in the high IL-6 expression group was significantly shorter compared with that in the low IL-6 expression group. In the present study, consecutive patients with PDAC who underwent surgery were included. As multidisciplinary treatment is the standard for pancreatic cancer, it could be considered that the inclusion of numerous patients who received preoperative chemotherapy (66%) may reflect the current status of pancreatic cancer treatment. Although it was considered that advanced age and preoperative chemotherapy may directly contribute to pancreatic stromal senescence, subgroup analysis demonstrated that IL-6 expression in PDAC stromal fibroblasts was not associated with any patient demographics and clinicopathological characteristics. Since pancreatic carcinogenesis is suggested to occur against a background of chronic inflammation (36-39), it was considered that cellular senescence of the pancreatic stroma begins at the pre-carcinogenesis stage. Although stromal depletion after preoperative chemotherapy has been reported (19), the present study found no evidence that preoperative chemotherapy directly induces further senescence in the cancer stroma. In summary, high expression intensity of IL-6 in the pancreatic cancer stromal fibroblasts was significantly associated with shorter survival after pancreatic cancer surgery. The presence of senescent fibroblasts and expression of SASP factors in the pancreatic cancer stroma may potentially serve as prognostic factors for pancreatic cancer.

The present *in vitro* studies demonstrated the successful establishment of pancreatic fibroblasts and confirmed the induction of cellular senescence and the expression of SASP factors in these fibroblasts following DNA damage by irradiation. Co-culture of pancreatic fibroblasts expressing SASP factors with pancreatic cancer cells revealed that the invasive, migratory and proliferative capacities of the cancer cells were significantly enhanced. The results of the *in vitro* analyses suggest that a microenvironment promoting cancer growth and spread is formed in pancreatic tissues subjected to X-ray irradiation, mimicking stress or DNA damage caused by chronic inflammation. Most forms of cellular senescence, such as replicative exhaustion, therapy-induced senescence or expression of oncogenic RAS, are associated with unrepaired DNA damage, similar to that caused by X-rays, and the choice of senescence inducer has been shown to have little effect on the senescent phenotype (8). Based on this finding, X ray irradiation was employed in the present study. To the best of our knowledge, no basic research on pancreatic cancer, a typical refractory solid tumor, has focused on cellular senescence and SASP in cancer stromal fibroblasts to clarify their effects on the tumor microenvironment and the promotion of cancer progression.

Numerous reports have demonstrated the role of CAFs in the tumor microenvironment. Several CAF markers have been documented, with the most commonly used including fibroblast activation protein α (FAP), αSMA and podoplanin (13-16). In the present study, increased FAP expression levels were observed in irradiated pancreatic fibroblasts (data not shown), which exhibited cellular senescence and the SASP. However, the expression of CAF markers is highly heterogeneous and varies significantly among CAF subpopulations (45). Furthermore, identifying CAFs remains challenging, and further investigation is needed to standardize CAF identification across studies. A limitation of the present study is that the overlap between senescent fibroblasts and CAFs was not assessed; therefore, it could not be determined whether they represent the same or distinct cell populations. Nevertheless, it remains possible that some senescent fibroblasts exhibiting SASP may function as CAFs within the tumor microenvironment to promote invasion and metastasis.

Cellular senescence is characterized by irreversible cell cycle arrest. Representative protein markers include

p16INK4a, p21 (Waf1/Clip1/Sdi1), p53 and Rb (3). Activation of p53 directly induces apoptosis and enhances the expression of p21, a cyclin-dependent kinase (CDK) inhibitor; by inhibiting CDKs, p21 activates Rb and suppresses the function of E2F, which regulates the transcription of genes that promote cell proliferation (3). E2F is responsible for the G_1-to-S phase transition of the cell cycle; its inhibition arrests cells in the G_1 phase (3). In parallel, p16INK4a inhibits CDK4/6, which also serves a role in G_1 progression. During cellular senescence, Rb remains constantly activated through these two CDK-inhibitory pathways. Although p21 and p16INK4a alone weakly activate Rb, their combined action robustly maintains Rb activation and arrests cell cycle progression (46). p16INK4a expression is extremely low in cells with normal proliferative potential and is nearly undetectable. However, its expression markedly increases when normal cells reach their mitotic limit or experience oncogenic stress, thereby inducing senescence (34,35). Therefore, p16INK4a is a key marker of cellular senescence.

The SASP comprises multiple factors, including IL-6, which may act synergistically within the cancer microenvironment. IL-6, a pleiotropic proinflammatory cytokine, has been shown to promote senescence and influence tumor formation (47,48). IL-6 is associated with DNA damage (and tumorigenic stress) induced senescence in keratinocytes, melanocytes, monocytes, fibroblasts and epithelial cells (47,49-51). According to previous reports, IL-6 affects tumor cells and the surrounding microenvironment by upregulating various genes (such as granulocyte-macrophage colony-stimulating factor, ILs, matrix metalloproteinase-2, nuclear factor erythroid 2-related factor 2, receptor for advanced glycation end-products and VEGF) and activating multiple tumor-promoting processes, such as angiogenesis and metastasis (52). The IL-6 signaling pathway is considered a key contributor to pancreatic cancer development. Through IL-6 expression, senescent fibroblasts can influence nearby cells expressing the IL-6 receptor (gp80) and gp130 signaling complex, such as epithelial and endothelial cells (8). IL-6 binding to its receptor activates Janus kinase 2 (JAK2), which transmits signals to the downstream STAT3 protein. STAT3 promotes pancreatic cancer progression by inducing genes such as cyclin D1 and Bcl-2, upregulating VEGF, promoting epithelial-mesenchymal transition and inhibiting dendritic cell-mediated immune responses (53). STAT3 is considered an oncogene owing to its widespread activation in cancer. In addition to JAK-STAT3, IL-6 also activates the Ras-mitogen-activated protein kinase (MAPK) and phosphoinositide-3-kinase (PI3K)-Akt pathways, which contribute to anti-apoptotic and tumorigenic effects (54). In various malignancies, including colorectal, renal, prostate, breast and ovarian cancer, as well as multiple myeloma and non-small cell lung cancer, increased serum IL-6 concentrations have been associated with advanced tumor stage and poor survival (52). In the present study, it was found that senescent pancreatic fibroblasts induced by X-ray irradiation exhibited simultaneous upregulation of multiple mRNA transcripts, including IL-6. A key limitation of the present study is the lack of a systematic evaluation of IL-6 in relation to other critical factors. This limitation arises from the inherent constraints of *in vitro* systems in recapitulating the complex tumor microenvironment, which is shaped by the dynamic interplay of various cell types and molecular signals. Furthermore, the SASP encompasses a broad array of factors, making it difficult to comprehensively assess SASP function. However, given that IL-6 signaling is widely recognized as a major contributor to pancreatic cancer progression, the present study focused on IL-6 as the most representative SASP factor. Future research on cellular senescence within the tumor microenvironment will enable a more complete evaluation of SASP function. Specifically, these include spatial gene expression analysis to visualize gene expression in specific regions of biological tissue and investigate the localization of SASP factors and the microenvironment in which SASP factors are released, as well as biological approaches such as creating animal models with specific SASP factors deleted to identify their functions and examine their effects on senescence and disease within the organism.

A previous report established a mouse model (p16-CreERT2-DTR-tdTomato) that enables the removal of p16-positive cells, showing positive results (55). In that study, non-alcoholic steatohepatitis (NASH) was induced by feeding mice a choline-deficient L-amino acid high-fat diet for 6 weeks. Removal of p16-positive cells during the final 3 weeks improved hepatic steatosis and inflammation. These findings indicate that NASH progression may be suppressed by eliminating p16-positive cells. Senescent cells have an apoptosis resistance mechanism similar to that of cancer cells, including high expression of the anti-apoptotic Bcl-2 family proteins. Based on the concept that senescent cells can be selectively eliminated by chemotherapy, various drugs have been screened, and the development of senolytic agents that specifically target senescent cells is advancing. Dasatinib plus quercetin, the first senolytic drug, has progressed to clinical trials for multiple diseases and has shown efficacy (56,57). In addition, studies have reported that the removal of senescent cells from atherosclerotic plaques (58) and the central nervous system (59) in mice suppresses the progression of age-related diseases. Other reports demonstrate the effectiveness of senolytic drugs via p53 activation, which promotes apoptosis in senescent cells (60,61). Most of these studies have targeted age-related diseases and excluded malignant tumors. Presently, no senolytic drugs have shown statistically significant effects in clinical trials involving living organisms. However, in the future, new therapies targeting malignant tumors by removing senescent cells may be developed.

Senescent fibroblasts in the cancer stroma produce various substances, such as SASP factors, that influence cancer progression. The present study demonstrated the presence of senescent fibroblasts in the pancreatic cancer stroma, with a positive correlation between p16 and IL-6 expression in fibroblasts. Furthermore, IL-6 expression in pancreatic cancer stromal fibroblasts was identified as a significant prognostic factor, along with lymph node metastasis, following pancreatic cancer surgery. Therefore, evaluating the presence of senescent cells and the expression of SASP factors in the pancreatic cancer stroma may be useful for predicting postoperative prognosis in patients with pancreatic cancer in the future.

Acknowledgements

The authors would like to thank Ms. Yasuyo Futakuchi and Ms. Kyoko Yoshida, the Medical Technologist of Gastrointestinal

Surgery, Kanazawa University, who provided technical support for the experiments and made significant contribution.

Funding

The present study was supported by the JSPS KAKENHI (grant no. JP23K08163).

Availability of data and materials

The data generated in the present study may be requested from the corresponding author.

Authors' contributions

YK, TM, YY, NI and SY designed and conceived the study. YK, TM and TS analyzed and interpreted the results and drafted the manuscript. TM and YY supervised this study. YK and IM collected the data. YE contributed to the establishment of pancreatic fibroblasts. TS, YY, NI and SY edited and revised the manuscript critically for intellectual content. All the authors have read and approved the final version of the manuscript. YK and TM confirm the authenticity of all the raw data.

Ethics approval and consent to participate

The present study followed the provisions of the Declaration of Helsinki and was approved by the Ethical Review Committee of Kanazawa University Hospital (approval no. 2016-318). Written informed consent was obtained from all participants for the anonymous use of resected specimens and clinical data.

Patient consent for publication

Not applicable.

Competing interests

The authors declare that they have no competing interests.

Authors' information

YK, 0000-0003-1941-9074; TM, 0000-0002-3771-0773; TS, 0009-0001-5490-8271; IM, 0000-0001-6023-7163; YE, 0000-0003-0785-2006; YY, 0000-0003-1326-4649; NI, 0000-0002-4241-5015; SY, 0000-0001-7465-5761.

References

1. Hayflick L and Moorhead PS: The serial cultivation of human diploid cell strains. Exp Cell Res 25: 585-621, 1961.
2. Campisi J and d'Adda di Fagagna F: Cellular senescence: When bad things happen to good cells. Nat Rev Mol Cell Biol 8: 729-740, 2007.
3. Ohtani N, Mann DJ and Hara E: Cellular senescence: Its role in tumor suppression and aging. Cancer Sci 100: 792-797, 2009.
4. Dimri GP, Lee X, Basile G, Acosta M, Scott G, Roskelley C, Medrano EE, Linskens M, Rubelj I and Pereira-Smith O, *et al*: A biomarker that identifies senescent human cells in culture and in aging skin in vivo. Proc Natl Acad Sci USA 92: 9363-9367, 1995.
5. Kuilman T, Michaloglou C, Mooi WJ and Peeper DS: The essence of senescence. Genes Dev 24: 2463-2479, 2010.
6. Harper JW and Elledge SJ: The DNA damage response: Ten years after. Mol Cell 28: 739-745, 2007.
7. Mallette FA and Ferbeyre G: The DNA damage signaling pathway connects oncogenic stress to cellular senescence. Cell Cycle 6: 1831-1836, 2007.
8. Coppé JP, Desprez PY, Krtolica A and Campisi J: The senescence-associated secretory phenotype: The dark side of tumor suppression. Annu Rev Pathol 5: 99-118, 2010.
9. Tchkonia T, Zhu Y, van Deursen J, Campisi J and Kirkland JL: Cellular senescence and the senescent secretory phenotype: Therapeutic opportunities. J Clin Invest 123: 966-972, 2013.
10. Muñoz-Espín D, Cañamero M, Maraver A, Gómez-López G, Contreras J, Murillo-Cuesta S, Rodríguez-Baeza A, Varela-Nieto I, Ruberte J, Collado M and Serrano M: Programmed cell senescence during mammalian embryonic development. Cell 155: 1104-1118, 2013.
11. Demaria M, Ohtani N, Youssef SA, Rodier F, Toussaint W, Mitchell JR, Laberge RM, Vijg J, Van Steeg H, Dollé ME, *et al*: An essential role for senescent cells in optimal wound healing through secretion of PDGF-AA. Dev Cell 31: 722-733, 2014.
12. Laberge RM, Awad P, Campisi J and Desprez PY: Epithelial-mesenchymal transition induced by senescent fibroblasts. Cancer Microenviron 5: 39-44, 2012.
13. Von Ahrens D, Bhagat TD, Nagrath D, Maitra A and Verma A: The role of stromal cancer-associated fibroblasts in pancreatic cancer. J Hematol Oncol 10: 76, 2017.
14. Kawase T, Yasui Y, Nishina S, Hara Y, Yanatori I, Tomiyama Y, Nakashima Y, Yoshida K, Kishi F, Nakamura M and Hino K: Fibroblast activation protein-α-expressing fibroblasts promote the progression of pancreatic ductal adenocarcinoma. BMC Gastroenterol 15: 109, 2015.
15. Tabola R, Zaremba-Czogalla M, Baczynska D, Cirocchi R, Stach K, Grabowski K and Augoff K: Fibroblast activating protein-α expression in squamous cell carcinoma of the esophagus in primary and irradiated tumors: The use of archival FFPE material for molecular techniques. Eur J Histochem 61: 2793, 2017.
16. Shindo K, Aishima S, Ohuchida K, Fujiwara K, Fujino M, Mizuuchi Y, Hattori M, Mizumoto K, Tanaka M and Oda Y: Podoplanin expression in cancer-associated fibroblasts enhances tumor progression of invasive ductal carcinoma of the pancreas. Mol Cancer 12: 168, 2013.
17. Su S, Chen J, Yao H, Liu J, Yu S, Lao L, Wang M, Luo M, Xing Y, Chen F, *et al*: CD10+GPR77+ Cancer-associated fibroblasts promote cancer formation and chemoresistance by sustaining cancer stemness. Cell 172: 841-856.e16, 2018.
18. Paulsson J, Rydén L, Strell C, Frings O, Tobin NP, Fornander T, Bergh J, Landberg G, Stål O and Östman A: High expression of stromal PDGFRβ is associated with reduced benefit of tamoxifen in breast cancer. J Pathol Clin Res 3: 38-43, 2016.
19. Miyashita T, Tajima H, Makino I, Okazaki M, Yamaguchi T, Ohbatake Y, Nakanuma S, Hayashi H, Takamura H, Ninomiya I, *et al*: Neoadjuvant chemotherapy with gemcitabine plus nab-paclitaxel reduces the number of cancer-associated fibroblasts through depletion of pancreatic stroma. Anticancer Res 38: 337-343, 2018.
20. Miyashita T, Tajima H, Gabata R, Okazaki M, Shimbashi H, Ohbatake Y, Okamoto K, Nakanuma S, Sakai S, Makino I, *et al*: Impact of extravasated platelet activation and podoplanin-positive cancer-associated fibroblasts in pancreatic cancer stroma. Anticancer Res 39: 5565-5572, 2019.
21. Lee JS, Yoo JE, Kim H, Rhee H, Koh MJ, Nahm JH, Choi JS, Lee KH and Park YN: Tumor stroma with senescence-associated secretory phenotype in steatohepatitic hepatocellular carcinoma. PLoS One 12: e0171922, 2017.
22. Harper EI, Sheedy EF and Stack MS: With great age comes great metastatic ability: Ovarian cancer and the appeal of the aging peritoneal microenvironment. Cancers (Basel) 10: 230, 2018.
23. Mori JO, Elhussin I, Brennen WN, Graham MK, Lotan TL, Yates CC, De Marzo AM, Denmeade SR, Yegnasubramanian S, Nelson WG, *et al*: Prognostic and therapeutic potential of senescent stromal fibroblasts in prostate cancer. Nat Rev Urol 21: 258-273, 2024.
24. Nakayama I: Therapeutic strategy for scirrhous type gastric cancer. Jpn J Clin Oncol 55: 860-870, 2025.
25. Yamamoto Y, Kasashima H, Fukui Y, Tsujio G, Yashiro M and Maeda K: The heterogeneity of cancer-associated fibroblast subpopulations: Their origins, biomarkers, and roles in the tumor microenvironment. Cancer Sci 114: 16-24, 2023.
26. Ministry of Education, Culture, Sports, Science and Technology, Ministry of Health, Labour and Welfare, and Ministry of Economy, Trade and Industry: Ethical guidelines for medical and biological research involving human subjects (In Japanese). https://www.mhlw.go.jp/content/000757566.pdf. 2021

27. Brierley JD, Gospodarowicz MK and Wittekind C: Union for International Cancer Control (UICC). TNM Classification of Malignant Tumors. 8th Edition. Wiley-Blackwell, 2017.
28. Tsuta K, Wistuba II and Moran CA: Differential expression of somatostatin receptors 1-5 in neuroendocrine carcinoma of the lung. Pathol Res Pract 208: 470-474, 2012.
29. Schmid HA, Lambertini C, van Vugt HH, Barzaghi-Rinaudo P, Schäfer J, Hillenbrand R, Sailer AW, Kaufmann M and Nuciforo P: Monoclonal antibodies against the human somatostatin receptor subtypes 1-5: Development and immunohistochemical application in neuroendocrine tumors. Neuroendocrinology 95: 232-247, 2012.
30. Roncoroni L, Elli L, Doneda L, Piodi L, Ciulla MM, Paliotti R and Bardella MT: Isolation and culture of fibroblasts from endoscopic duodenal biopsies of celiac patients. J Transl Med 7: 40, 2009.
31. Seluanov A, Vaidya A and Gorbunova V: Establishing primary adult fibroblast cultures from rodents. J Vis Exp 5: 2033, 2010.
32. Livak KJ and Schmittgen TD: Analysis of relative gene expression data using real-time quantitative PCR and the 2(-Delta Delta C(T)) Method. Methods 25: 402-408, 2001.
33. Rasband WS: ImageJ, U.S. National Institutes of Health, Bethesda, MD, 2011. http://imagej.nih.gov/ij
34. Hara E, Smith R, Parry D, Tahara H, Stone S and Peters G: Regulation of p16CDKN2 expression and its implications for cell immortalization and senescence. Mol Cell Biol 16: 859-867, 1996.
35. Serrano M, Lin AW, McCurrach ME, Beach D and Lowe SW: Oncogenic ras provokes premature cell senescence associated with accumulation of p53 and p16INK4a. Cell 88: 593-602, 1997.
36. Raimondi S, Lowenfels AB, Morselli-Labate AM, Maisonneuve P and Pezzilli R: Pancreatic cancer in chronic pancreatitis; aetiology, incidence, and early detection. Best Pract Res Clin Gastroenterol 24: 349-358, 2010.
37. Qiu D, Kurosawa M, Lin Y, Inaba Y, Matsuba T, Kikuchi S, Yagyu K, Motohashi Y and Tamakoshi A; JACC Study Group: Overview of the epidemiology of pancreatic cancer focusing on the JACC study. J Epidemiol 15 (Suppl II): S157-S167, 2005.
38. Iodice S, Gandini S, Maisonneuve P and Lowenfels AB: Tobacco and the risk of pancreatic cancer: A review and meta-analysis. Langenbecks Arch Surg 393: 535-545, 2008.
39. Tramacere I, Scotti L, Jenab M, Bagnardi V, Bellocco R, Rota M, Corrao G, Bravi F, Boffetta P and La Vecchia C: Alcohol drinking and pancreatic cancer risk: A meta-analysis of the dose-risk relation. Int J Cancer 126: 1474-1486, 2010.
40. Gosavi R, Jaya J, Yap R, Narasimhan V and Ooi G: Obesity and gastrointestinal cancer: A converging epidemic with surgical consequence. Eur J Surg Oncol 51: 110358, 2025.
41. Cuomo RE: Distinct somatic mutation profiles in colon cancer by behavioral comorbidity. Future Sci OA 11: 2561501, 2025.
42. Wang J, Qiu K, Zhou S, Gan Y, Jiang K, Wang D and Wang H: Risk factors for hepatocellular carcinoma: An umbrella review of systematic review and meta-analysis. Ann Med 57: 2455539, 2025.
43. Ni L, Liu Z, Xiang L, Li Y and Zhang Y: Comprehensive evaluation of risk factors for LNM and distant metastasis in patients with NSCLC. Sci Rep 15: 30809, 2025.
44. Min SK, You Y, Choi DW, Han IW, Shin SH, Yoon S, Jung JH, Yoon SJ and Heo JS: Prognosis of pancreatic head cancer with different patterns of lymph node metastasis. J Hepatobiliary Pancreat Sci 29: 1004-1013, 2022.
45. Nurmik M, Ullmann P, Rodriguez F, Haan S and Letellier E: In search of definitions: Cancer-associated fibroblasts and their markers. Int J Cancer 146: 895-905, 2020.
46. Ohtani N, Imamura Y, Yamakoshi K, Hirota F, Nakayama R, Kubo Y, Ishimaru N, Takahashi A, Hirao A, Shimizu T, *et al*: Visualizing the dynamics of p21(Waf1/Cip1) cyclin-dependent kinase inhibitor expression in living animals. Proc Natl Acad Sci USA 104: 15034-15039, 2007.
47. Kuilman T, Michaloglou C, Vredeveld LC, Douma S, van Doorn R, Desmet CJ, Aarden LA, Mooi WJ and Peeper DS: Oncogene-induced senescence relayed by an interleukin-dependent inflammatory network. Cell 133: 1019-1031, 2008.
48. Ancrile B, Lim KH and Counter CM: Oncogenic Ras-induced secretion of IL6 is required for tumorigenesis. Genes Dev 21: 1714-1719, 2007.
49. Coppé JP, Patil CK, Rodier F, Sun Y, Munoz DP, Goldstein J, Nelson PS, Desprez PY and Campisi J: Senescence-associated secretory phenotypes reveal cell-nonautonomous functions of oncogenic RAS and the p53 tumor suppressor. PLoS Biol 6: 2853-2868, 2008.
50. Lu SY, Chang KW, Liu CJ, Tseng YH, Lu HH, Lee SY and Lin SC: Ripe areca nut extract induces G1 phase arrests and senescence-associated phenotypes in normal human oral keratinocyte. Carcinogenesis 27: 1273-1284, 2006.
51. Sarkar D, Lebedeva IV, Emdad L, Kang DC, Baldwin AS Jr and Fisher PB: Human polynucleotide phosphorylase (hPNPaseold-35): A potential link between aging and inflammation. Cancer Res 64: 7473-7478, 2004.
52. Holmer R, Goumas FA, Waetzig GH, Rose-John S and Kalthoff H: Interleukin-6: A villain in the drama of pancreatic cancer development and progression. Hepatobiliary Pancreat Dis Int 13: 371-380, 2014.
53. Song M, Tang Y, Cao K, Qi L and Xie K: Unveiling the role of interleukin-6 in pancreatic cancer occurrence and progression. Front Endocrinol (Lausanne) 15: 1408312, 2024.
54. Ara T and Declerck YA: Interleukin-6 in bone metastasis and cancer progression. Eur J Cancer 46: 1223-1231, 2010.
55. Omori S, Wang TW, Johmura Y, Kanai T, Nakano Y, Kido T, Susaki EA, Nakajima T, Shichino S, Ueha S, *et al*: Generation of a p16 reporter mouse and its use to characterize and target $p16^{high}$ cells in vivo. Cell Metab 32: 814-828.e6, 2020.
56. Hickson LJ, Langhi Prata LGP, Bobart SA, Evans TK, Giorgadze N, Hashmi SK, Herrmann SM, Jensen MD, Jia Q, Jordan KL, *et al*: Senolytics decrease senescent cells in humans: Preliminary report from a clinical trial of dasatinib plus quercetin in individuals with diabetic kidney disease. EBiomedicine 47: 446-456, 2019.
57. Farr JN, Atkinson EJ, Achenbach SJ, Volkman TL, Tweed AJ, Vos SJ, Ruan M, Sfeir J, Drake MT, Saul D, *et al*: Effects of intermittent senolytic therapy on bone metabolism in postmenopausal women: A phase 2 randomized controlled trial. Nat Med 30: 2605-2612, 2024.
58. Bussian TJ, Aziz A, Meyer CF, Swenson BL, van Deursen JM and Baker DJ: Clearance of senescent glial cells prevents tau-dependent pathology and cognitive decline. Nature 562: 578-582, 2018.
59. Childs BG, Baker DJ, Wijshake T, Conover CA, Campisi J and van Deursen JM: Senescent intimal foam cells are deleterious at all stages of atherosclerosis. Science 354: 472-477, 2016.
60. Paez-Ribes M, González-Gualda E, Doherty GJ and Muñoz-Espín D: Targeting senescent cells in translational medicine. EMBO Mol Med 11: e10234, 2019.
61. Baar MP, Brandt RMC, Putavet DA, Klein JDD, Derks KWJ, Bourgeois BRM, Stryeck S, Rijksen Y, van Willigenburg H, Feijtel DA, *et al*: Targeted apoptosis of senescent cells restores tissue homeostasis in response to chemotoxicity and aging. Cell 169: 132-147.e16, 2017.